Chapter 5

Transmission Infrared Absorption Spectroscopy

5.1 Introduction

As has been described in the preceding chapters, the Ge(111) surface can be alkyl-terminated in a method very similar to the thoroughly investigated Si(111) surface. However, while the process does produce alkyl-terminated surfaces with electrical properties superior to those of the oxide, the lack of a mild, anisotropic etchant analogous to NH_4F, is a drawback to the production of a surface as well ordered as that of alkyl-terminated Si(111). The methyl-terminated Si(111) surface prepared though the halogenation/alkylation procedure has been well characterized by infrared absorption spectroscopy (IRAS) and scanning tunneling microscopy (STM) to show that every top silicon atom may be capped by a methyl group, with the Si-C bond directed normal to the surface plane.[1–4] While longer chain hydrocarbons groups, such as octadecyl, have been grafted to crystalline Ge and shown to display a crystallinity indicative of a well-ordered overlayer, evidence of a similar level of order at the Ge-C bond has not yet been reported.[5–7]. The work described in this chapter characterizes the alkyl-terminated Ge(111) surface through transmission IRAS to indicate that the methyl-terminated Ge(111) surface can be well ordered, with the Ge-C bond directed normal to the surface, as depicted in Figure 5.1.

Figure 5.1: Methyl group oriented normal to the Ge(111) surface

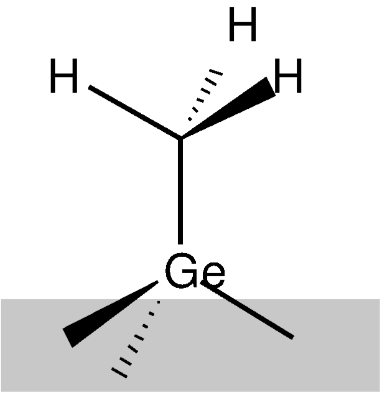

5.1.1 Background

Transmission

Germanium transmits light of wavelengths between 2 and 14 μm, so it is a commonly used infrared optical material often used in internal reflection experiments.[8] Silicon may also be used as an infrared optical material, however multiphonon absorption limits the useful spectral range to 1 – 6.7 μm.[9] Transmission IR absorption spectroscopy experiments (TIRAS), in the arrangement depicted in Figure 5.2, have been used for the study of monolayers on silicon wafers because the optical path within the crystal bulk is a single pass through a 500 μm wafer rather than the centimeter or greater in a multiple internal reflection configuration, so that the spectral range is no longer confined by bulk absorption.

While the phonon absorption of Ge does not limit the spectral range to the degree observed in Si, there are other reasons to use TIRAS. ATR requires specially crafted multiple internal reflection elements (IRE), which limits the sample availability. Comparison between different samples is also complicated because of the integral role the IRE has in the optical path, so that the precision of alignment required is difficult to achieve. TIRAS requires only standard semiconductor wafers and has a simplified optical path, so that comparisons between samples is more easily achieved.

Orientation of vibrational modes relative to the surface plane can be measured by controlling the angle of incidence of the IR on the wafer. At the Brewster angle, the reflected beam path is parallel to the electric field of the transmitted p-polarized light. There can be no emission from the surface as a result, so the reflected beam intensity is zero and all p-polarized light is transmitted, while s-polarized light is largely reflected, as indicated in Figure 5.2. The electric field vector of the transmitted light is at an angle to the wafer surface, with components both perpendicular and parallel to the surface. Vibrational modes that are perpendicular to the surface may absorb energy from the component of the p-polarized light in the same orientation, and surface parallel vibrational modes similarly absorb the parallel component, so that all modes are visible in the collected absorption spectrum. If the angle of incidence is changed to be closer to normal incidence, the component of the transmitted p-polarized light that may be absorbed by the vibrational mode perpendicular to the surface is reduced relative to the parallel component because the electric field vector is more parallel to the surface. In addition, the transmission ratio of s-polarized light to p-polarized light is increased, and electric field vector is parallel to the surface. As a result, the surface parallel vibrational modes are observed in the absorption spectra while the perpendicular modes are not.

External Reflection

In contrast to the ATR technique, external reflection measurements involve the light reflected off the surface of the higher refractive index material. While external reflection spectroscopy has traditionally been used to study adsorbed layers on metals, it may also be used for semiconducting and dielectric materials such as silicon of germanium.[10–12] Unfortunately, the same reflection/transmission properties that make TIRAS possible lead to a reflected beam that has very low power, resulting in a very low signal-to-noise ratio. However, the method does possess some desirable aspects: it does not require the special substrate geometries necessary for the more commonly used ATR technique; and the absorption spectra are highly polarization dependent, so that detailed structural information may be obtained. The overlap of the electric field vector of incident *p*-polarized light with the transition dipole moment vector of vibrations both parallel and perpendicular to the surface in the X-Y plane leads to two absorption components, A^x and A^z, respectively. One of the corresponding electric field components of the reflected beam must be out of phase while the other is in phase (see Figure 5.3), so that A^x and A^z will have opposite signs. Below the Brewster's angle, the reflected *p*-polarized light is in phase with the incident light and the A^z bands are positive while the A^x bands are negative (greater reflected power at that energy). The signs of the absorption components change as the angle of incidence is greater than the Brewster's angle. While the opposing signs of the absorption components can lead to complicated spectra for vibrational modes at an acute angle off the surface normal and would require simulations for interpretation, the simple geometry of the methyl groups as depicted in Figure 5.1 on page 113 would lead to distinct absorption bands composed wholly of either A^x or A^z.[13,14]

Figure 5.2: IR beam and sample wafer geometry for TIRAS

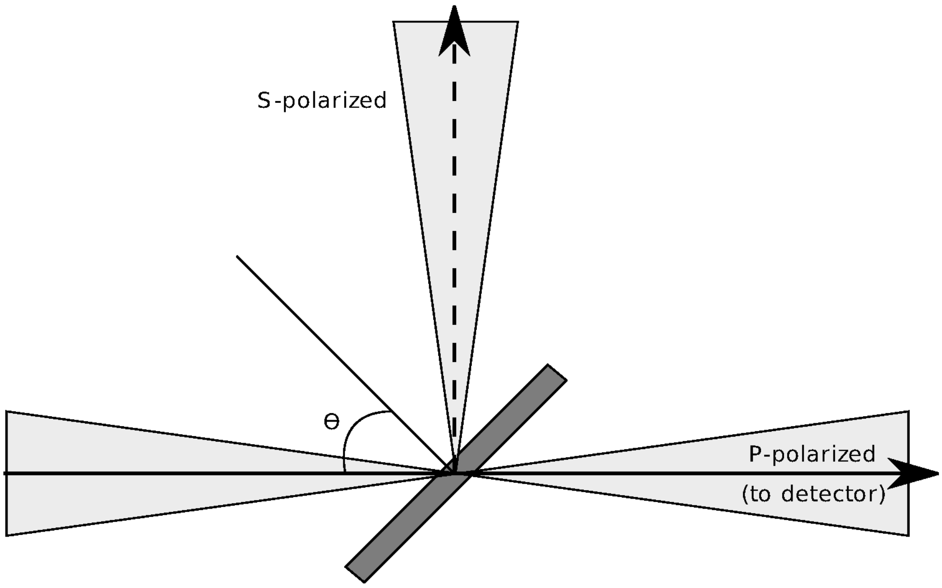

Figure 5.3: Beam and polarization geometry of IR radiation encountering dielectric surface

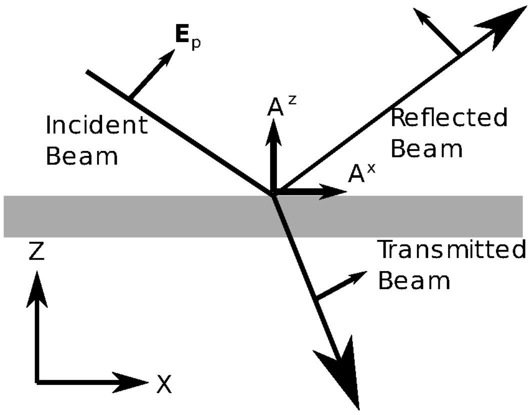

5.2 Experimental

Transmission infrared absorption spectroscopy was performed with a Nicolet 6700 FTIR, equipped with a custom-built accessory that held the sample upright on one edge, with the surface normal at a fixed angle, θ, of either 30° or 74° with respect to the path of the incident beam. For each stable sample, 3–5 single beam spectra of 1000 scans each were collected with a thermoelectrically cooled deuterated triglycine sulfate (DTGS) detector at a resolution of 4 cm^{-1}, a resolution which minimized the interference pattern produced by internal reflections. For less chemically stable surfaces, single-beam spectra of only 500 or 200 hundred scans were collected for etched surfaces. All spectra were converted to absorption spectra using other spectra collected the same day as background. The elapsed time between the sample and background spectra was minimized to avoid baseline distortion and imperfect subtraction of optical component absorptions due to spectrometer drift. Absorbance spectra were corrected for atmospheric CO_2 and H_2O absorption peaks. Because the background and sample spectra could not usually be collected from the same wafer within an allowable time-span, weak, broad signals below approximately 1000 cm^{-1} were difficult to distinguish from bulk absorptions or the artifacts previously mentioned.

External reflectance spectroscopy was performed with a variable angle reflectance accessory (Seagull, Harrick Scientific) and a polarizer to linearly polarize the incident beam parallel to the plane of incidence. In order to suppress multiple reflections, the sample wafers were single-side polished. So that no reflection from a supporting surface would interfere with the measurement, the samples were held by the edges and unsupported on the bottom. The low throughput of the setup required the collection of 5,000 scans for a single-beam spectrum.

5.3 Results

5.3.1 Methyl-Terminated Ge(111) Surfaces

Figure 5.4 displays a CD_3-Ge(111) sample against a CH_3-Ge(111) background. Both surfaces had been prepared through the bromination/methylation of HF-etched surfaces that had been pre-treated with the H_2O_2 anisotropic etch. The negative peaks at 1232 cm^{-1} and 755 cm^{-1} are due to the CH_3 groups of the background sample, the positive peaks at 2121 cm^{-1}, 951 cm^{-1}, and 577 cm^{-1} are due to the $\nu_s(CD_3)$, $\sigma_s(CD_3)$, and $\rho(CD_3)$ modes, respectively, of CD_3 groups. The higher energy modes in both sample and background disappear as θ is changed from 74° (lower spectrum) to 30° (upper spectrum), indicating those vibrational modes are normal to the surface plane, as would be expected for a methyl group bonded to the Ge(111) 1×1 surface.

Figure 5.4: CD_3-Ge(111) vs CH_3-Ge(111)

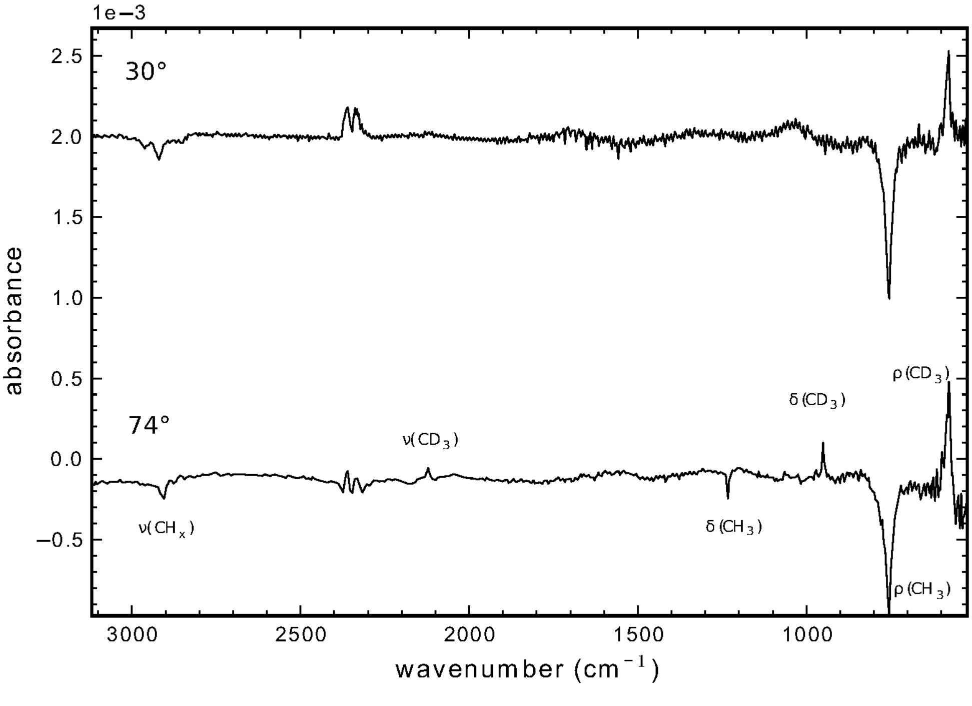

Further confirmation of the sensitivity of the absorption bands to the orientation of the electric field of the incident radiation can be seen in the external reflectance spectra of Figure 5.5, collected at $\theta = 67°$ off normal incidence. Because the angle of incidence is below the Brewster angle for both Si and Ge, a positive absorption is due to vibrational modes that are either perpendicular to the surface and present in the sample, or parallel to the surface and present in the background.[12] The inverse is true for the negative peaks. The upper spectrum is of a CH_3-Si(111) surface with H-Si(111) as background. The positive peak at 627 cm^{-1} is attributable to the Si-H bending mode of the background, while the positive peak at 1257 cm^{-1} and the negative peak at 757 cm^{-1} are attributable to the CH_3 umbrella mode and rocking mode, respectively.[1] The lower spectrum is of CH_3-Ge(111) with a rinsed oxide as background, so while there is no peak analogous to the H-Si(111) mode, the two CH_3 modes are present. The signs of the CH_3 absorption bands indicate that for both CH_3-Si(111) and CH_3-Ge(111), the methyl groups are oriented normal to the surface.

Figure 5.5: External reflectance spectra of CH_3-Si(111) and CH_3-Ge(111)

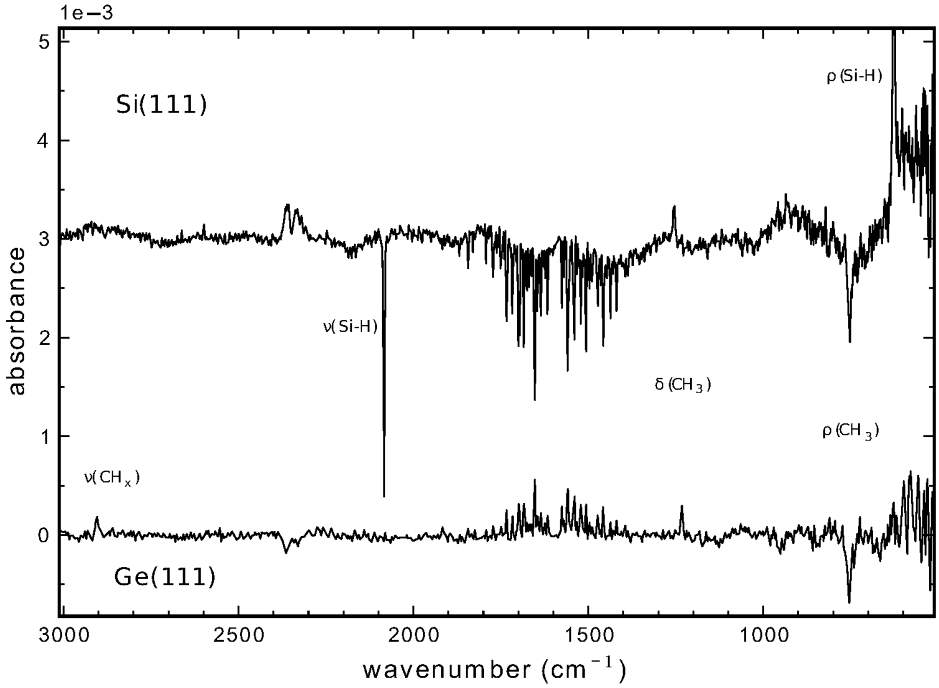

The halogenation/alkylation procedure reliably produces hydrophobic surfaces with little or no oxide, but the quality of the monolayer can depend strongly upon the initial etching method. The spectra presented in Figure 5.6 on page 124 are representative of the variation. The upper spectrum is of a sample that had been prepared by exposure of a Cl-Ge(111) surface, generated by etching with 6.0 M HCl, to a CD_3MgI solution. There is some evidence of the deuterated methyl group in the form of the $\nu_s(CD_3)$ mode at 2121 cm^{-1}, but the dominant peaks are not related to the desired monolayer and the spectrum does not give evidence of a methyl monolayer. The lower spectrum is of a surface prepared by etching with 6.0 M HBr, then exposure to CH_3MgI solution. The $\sigma_s(CH_3)$ mode at 1232 cm^{-1} and the $\rho(CH_3)$ mode at 755 cm^{-1} are clearly apparent, indicative of a methyl-terminated Ge surface.

If the samples are prepared from HF-etched surfaces, but are not pre-treated with the anisotropic etchant, the spectra resemble the upper spectrum of Figure 5.6 in that there is no clear evidence of the methyl vibrational modes. Conversely, if the HCl-etched surfaces are exposed to Br_2 vapor prior to methylation, the IR spectra of the resulting surfaces indicate well-ordered methyl monolayers, as seen in Figure 5.7. A mixture of 6.0 M NH_4Cl and 6.0 M HF could, after exposure to Br_2 vapor, also be used to produce well ordered CH_3-Ge(111) surfaces, which are shown in Figure 5.8. The variations on the general halogenation/alkylation procedure that were attempted, and their success as determined by TIRAS, are summarized in Table 5.1 on page 128. Increasing the concentration of the HF etchant to 12.0 M reduced the etching time required for the production of a hydrophobic surface, but gave results otherwise similar to the procedures involving 6.0 M HF(aq).

The absorption peak positions observed for CH_3- and CD_3-terminated surfaces are collected in Table 5.2. As can be seen both in the table and in Figure 5.9, the absorption peaks are shifted to a lower energy on Ge(111) compared to Si(111), but are otherwise similar.

Figure 5.6: CH_3-Ge(111) derived from surfaces etched with 6.0 M HCl or HBr, but not exposed to Br_2 vapor

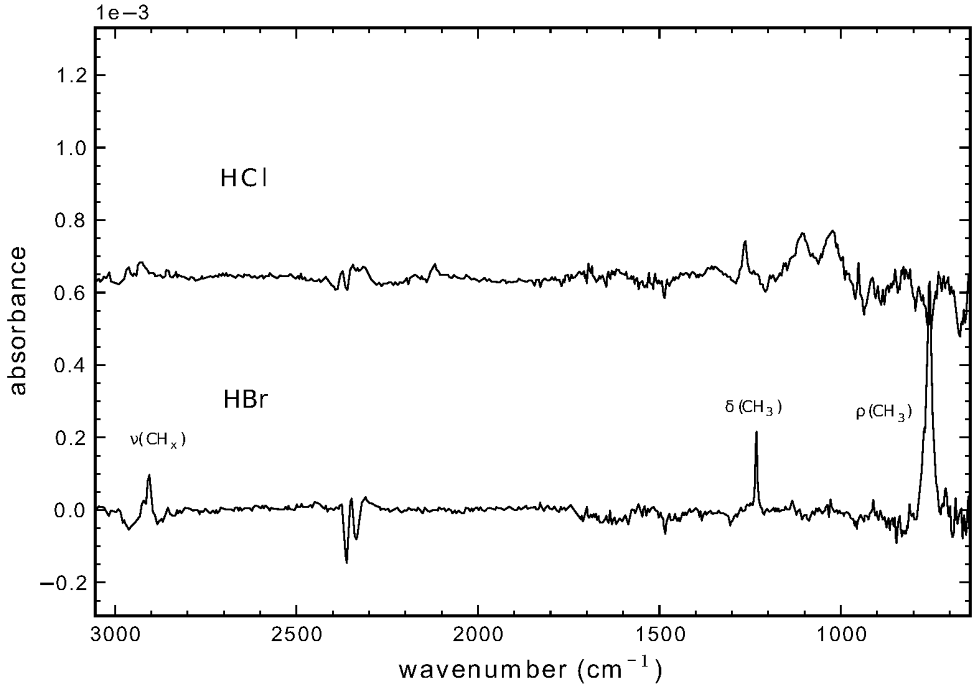

Figure 5.7: CH_3-Ge(111) derived from surfaces etched with 6.0 M HCl then exposed to Br_2 vapor

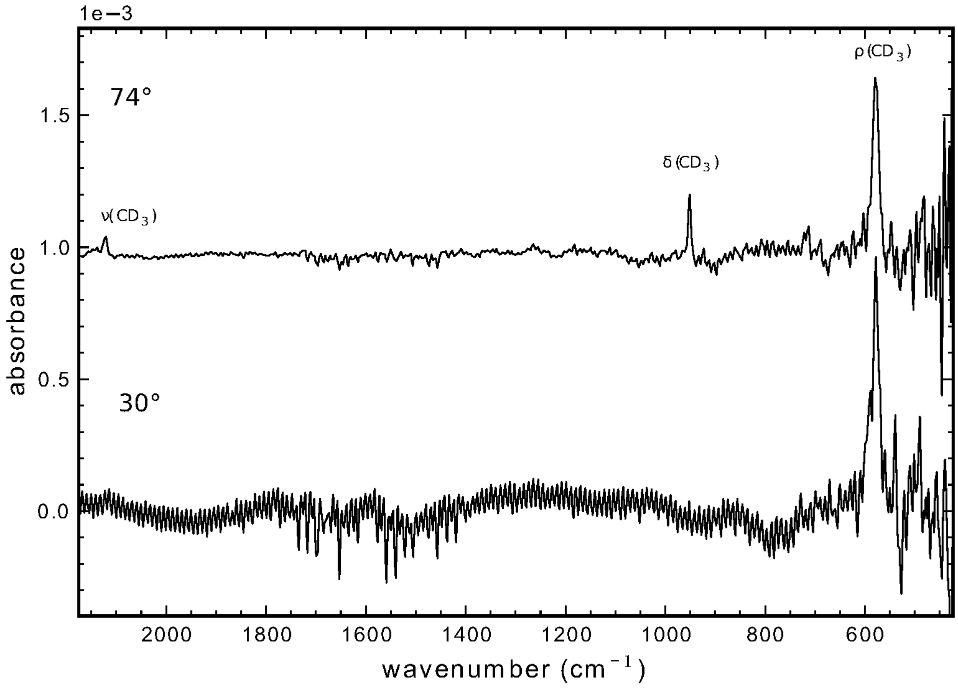

Figure 5.8: CH_3-Ge(111) derived from surfaces etched with NH_4Cl−HF mixture then exposed to Br_2 vapor

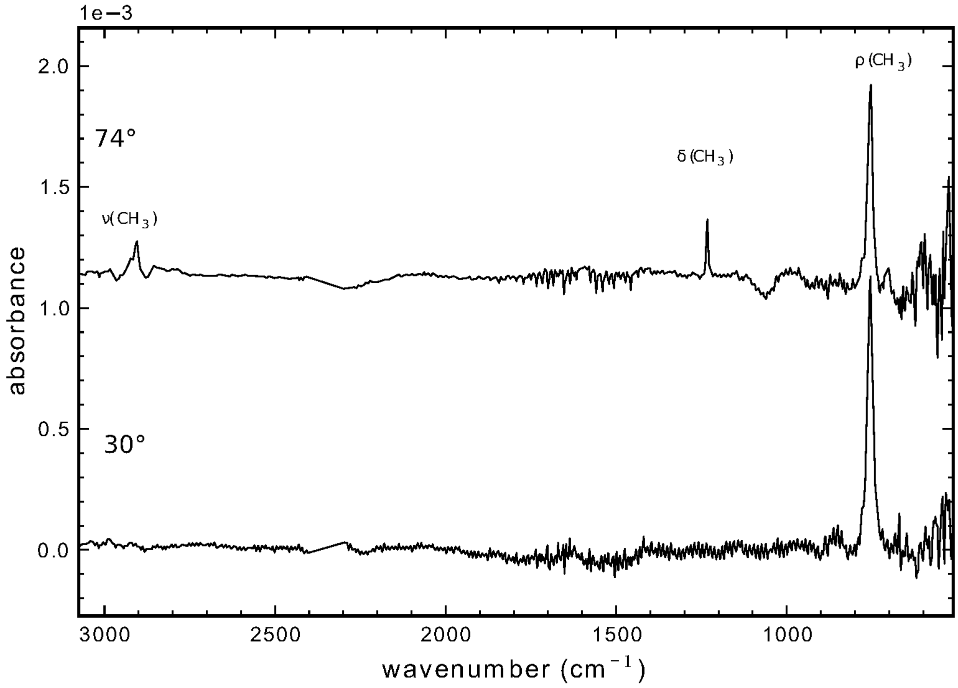

Figure 5.9: CD_3-Si(111) and CD_3-Ge(111)

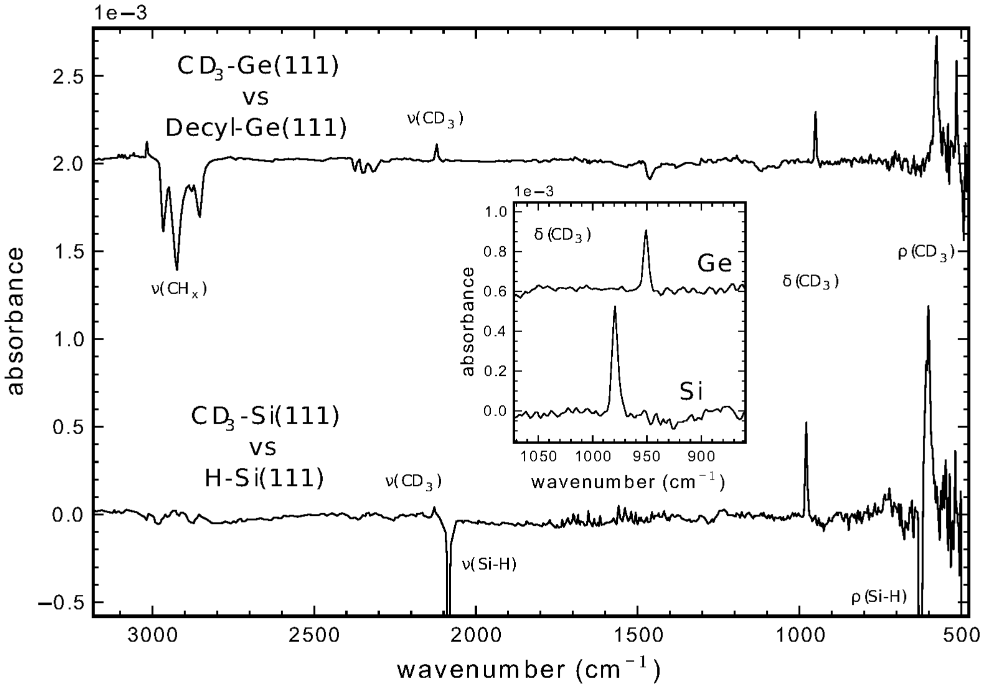

Table 5.1: Methylation Procedures

step number	process	surface type	success[a]
1	1-3 s Superoxol etch	GeO_x	
2	3-6 min 6.0 M HF	H-Ge(111)	
3	15-30 s Br_2 exposure	Br-Ge(111)	
4	3-12 h CH_3MgX (ether)	CH_3-Ge(111)	Y
1	20-25 min 6.0 M HF	H-Ge(111)	
2	15-30 s Br_2 exposure	Br-Ge(111)	
3	3-12 h CH_3MgX (ether)	CH_3-Ge(111)	N
1	20-25 min 6.0 M HCl	Cl-Ge(111)	
2	15-30 s Br_2 exposure	Br-Ge(111)	
3	3-12 h CH_3MgX (ether)	CH_3-Ge(111)	Y
1	20-25 min 6.0 M HCl	Cl-Ge(111)	
2	3-12 h CH_3MgX (ether)	CH_3-Ge(111)	N
1	1-3 s 6.0 M HBr	Br-Ge(111)	
2	3-12 h CH_3MgX (ether)	CH_3-Ge(111)	Y

[a] as determined by the presence of clear IR absorption peaks

5.3.2 Etched Surfaces

Samples that were not uniformly hydrophobic after etching did not become hydrophobic upon the completion of the alkylation procedure, and were seen with XPS to have varying but significant amounts of oxide. Samples that were etched for longer than was required to become hydrophobic became less hydrophobic as judged by the adhesion of the etching solution to the wafer surface. This is in general agreement with what has been observed on HF(aq) etching of Ge(100).[6] This effect was particularly noticeable in the case of surfaces treated with the Superoxol etchant. The etching times noted in Table 5.1 were adjusted to maximize the hydrophobicity as observed by the wetting of the surface by the etchant. The use of a H_2O_2 & HF-based etchant has some similarity to the sequential H_2O_2 then HF(aq) treatment used by others, however the sequential method resulted in surfaces indistinguishable from HF-only method.[15] The use of 3.3 M HCl(aq) is cited in the literature, but it required etching times greater then 30 min, and the etchant adhered to the surface non-uniformly.[16] Pretreatment of the sample with Superoxol etch prior to 3.3 M HCl(aq) resulted in a surface that remained uniformly hydrophilic for at least 45 min.

Hydrofluoric etchant

The unstable nature of the H-Ge(111) surface made it difficult to collect quantitative spectra, however absorptions attributable to Ge-H stretching modes were usually observed for HF-etched surfaces, with the notable exception of surfaces that were etched with the H_2O_2-based etchant prior to etching with 6.0 M HF(aq), a procedure henceforth referred to as Superoxol-6. This is demonstrated in Figure 5.10, which shows spectra of two 6.0 M HF(aq) etched surfaces, the upper of which had been treated with the H_2O_2-based etch just prior and shows no meaningful absorption bands. The lower spectrum shows a clear peak at 2040 cm^{-1}, attributable to the ν(Ge-H) stretch.[17–19] If the HF concentration is increased to 12.0 M, the Ge-H stretching is observed for surfaces both treated and not treated with Superoxol etch. In addition to the stretching mode absorption, there is another absorption at 560 cm^{-1}, shown in Figure 5.11, that is more noticeable in the sample that had been treated with Superoxol etch, but may be present in the HF-only sample as well.

The 560 cm^{-1} peak is less stable than the ν(Ge-H), and is entirely gone within ten minutes. If the peak at 560 cm^{-1} is initially present on the surface treated with the anisotropic etchant and then 6.0 M HF(aq), but is simply too air-sensitive to be measured, a hydrocarbon film may help protect it from moisture to extend the lifetime. The results of adding 2,4-dimethylpentane to the 6.0 M HF(aq) etchant are shown in Figure 5.12. Both spectra are of the same sample, but the background of the upper spectrum is the sample after it had been allowed to sit undisturbed in the spectrometer for 50 min. The background of the lower spectrum is the sample after sonication in detergent to restore a cleanly hydrophilic surface. The peak at 560 cm^{-1} does not coincide with the (C-H) modes in the lower spectrum. This peak is tentatively assigned to the rocking mode, ρ(Ge-H), analogous to that seen in H-Si(111)[20–22]

Hydrochloric and Hydrobromic Etchants

Surfaces treated with HCl(aq) or HBr(aq) did not show any absorption bands within the available spectral window, aside from adventitious hydrocarbon C-H stretching modes near 3000 cm^{-1}, which varied in intensity between samples. XP spectra confirmed the presence of the halogen at the surface, but the vibrational modes were too low in energy for the instrumentation used.

Ge(111) surfaces that had been treated with HCl(aq) or HBr(aq) did not show any infrared absorption bands within the available spectral window, aside from adventitious hydrocarbon C-H stretching modes near 3000 cm^{-1}, which varied in intensity between samples. XP spectra of surfaces etched with 6.0 M HCl(aq) and exposed to Br_2 showed evidence of both Cl and Br, but the Cl peaks were not intense enough to be quantified. After Br_2 exposure, the fractional monolayer coverage of Br was calculated from the XP spectra to be 1.0 ± 0.1 for the surfaces etched with only 6.0 M HF(aq), 1.1 ± 0.1 for the surfaces etched with Superoxol-6, and 0.5 ± 0.1 for the surfaces etched with 6.0 M HCl(aq).

Figure 5.10: 6.0 M HF(aq)-etched Ge(111) at 74° incidence

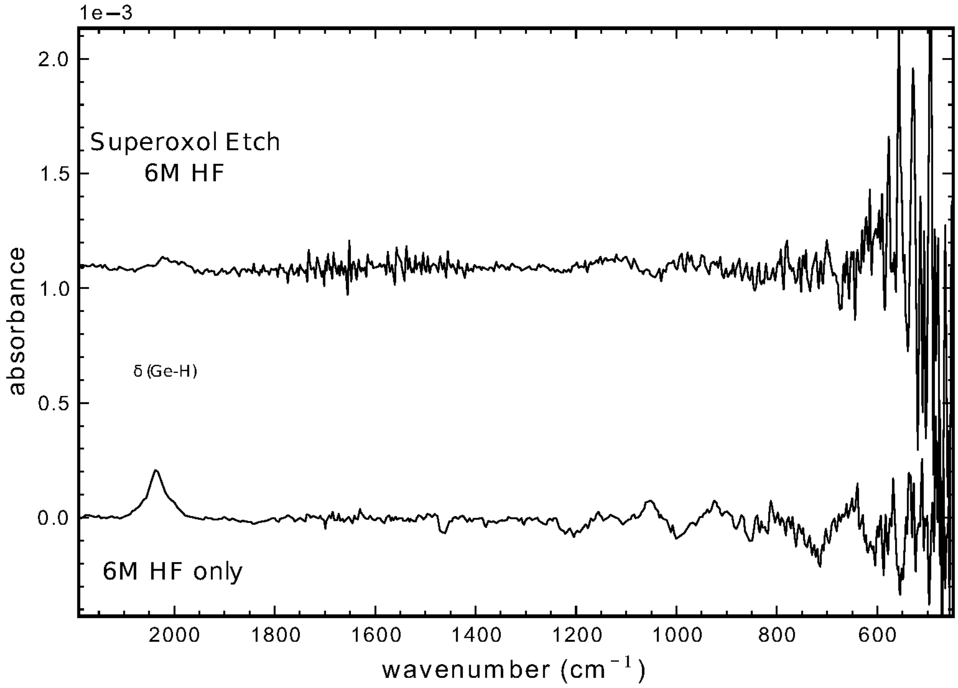

Figure 5.11: 12.0 M HF(aq)-etched Ge(111) at 74° incidence

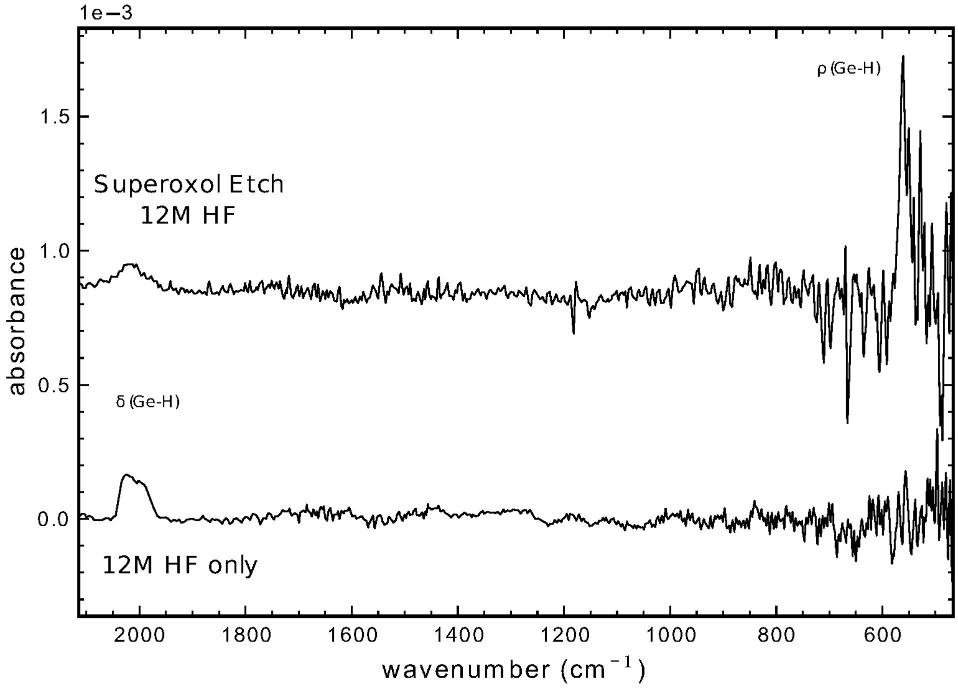

Figure 5.12: Effect of hydrocarbon in 6.0 M HF etchant

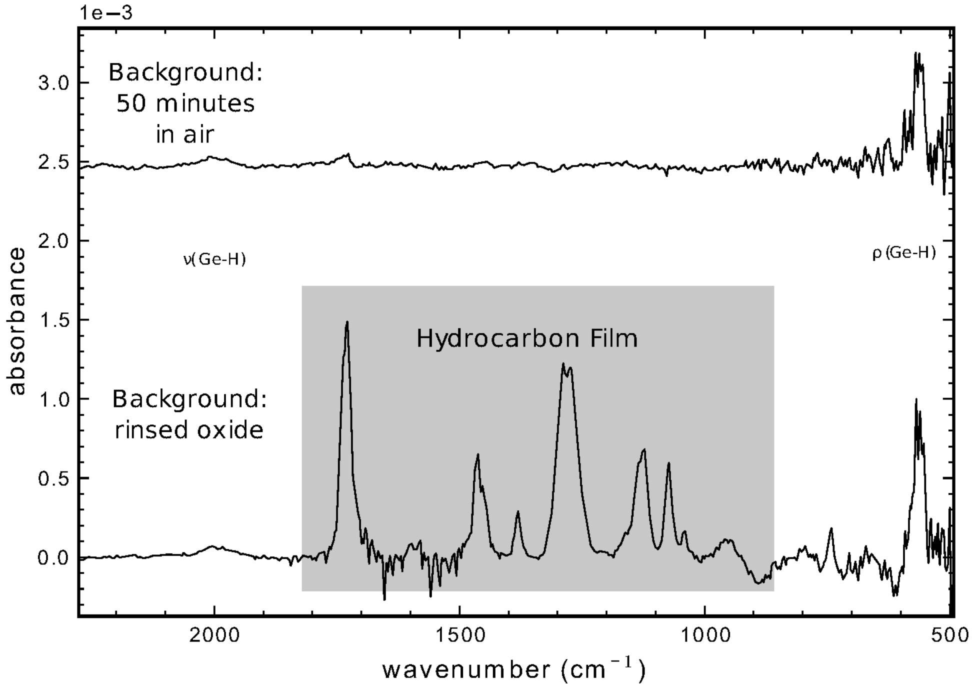

5.3.3 Decyl-Terminated Surfaces

The C-H stretching region of two $C_{10}H_{21}$-Ge(111) samples measured at 74° incidence is shown in 5.14. The top spectrum was prepared from a surface etched with the H_2O_2-based anisotropic etchant and the lower spectrum was prepared from a surface etched with 6.0 M HF only. The absorption peak positions and intensities match what has been established for similar monolayers on Au or Si surfaces, so the peaks at at 2854 cm^{-1} and 2924 cm^{-1} may be assigned to symmetric and antisymmetric methylene stretching modes, $\nu_s(CH_2)$ and $\nu_{as}(CH_2)$.[12,23,24] The peaks at 2879 cm^{-1} and 2966 cm^{-1} may be assigned to the symmetric and antisymmetric methyl stretching modes, $\nu_s(CH_3)$ and $\nu_{as}(CH_3)$. Figure 5.13 displays the same samples, measured at 30° incidence. There is a noticeable reduction in the $\nu(CH_3)$ modes. The features above 3000 cm^{-1} are artifacts due to atmospheric methane, and do not have any relation to the surface.

Figure 5.13: ν(C-H) region of $C_{10}H_{21}$-Ge(111) at 30° incidence

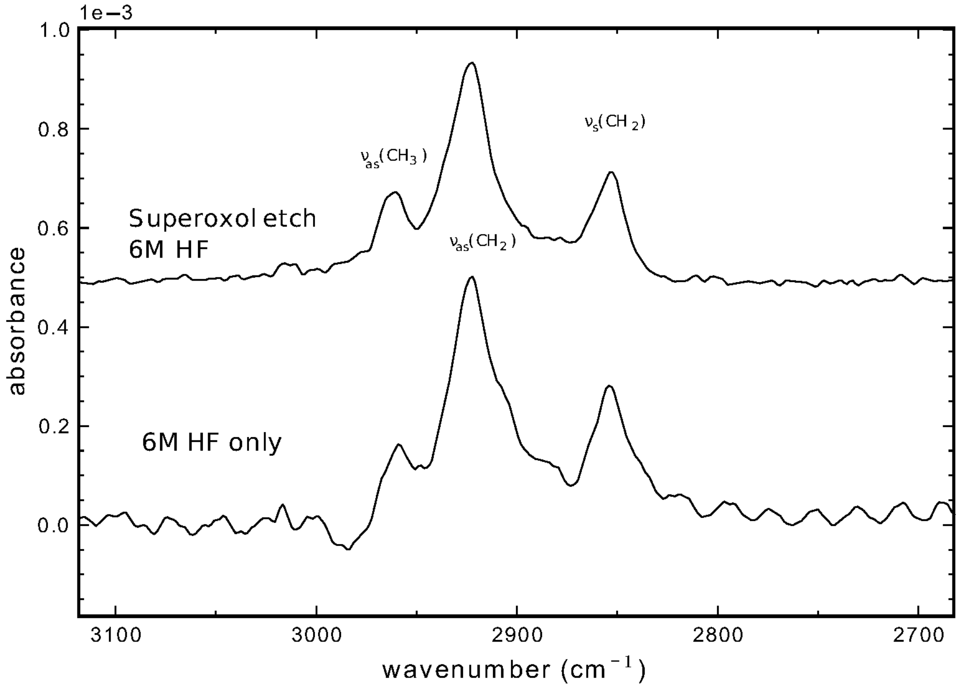

Figure 5.14: ν(C-H) region of $C_{10}H_{21}$-Ge(111) at 74° incidence

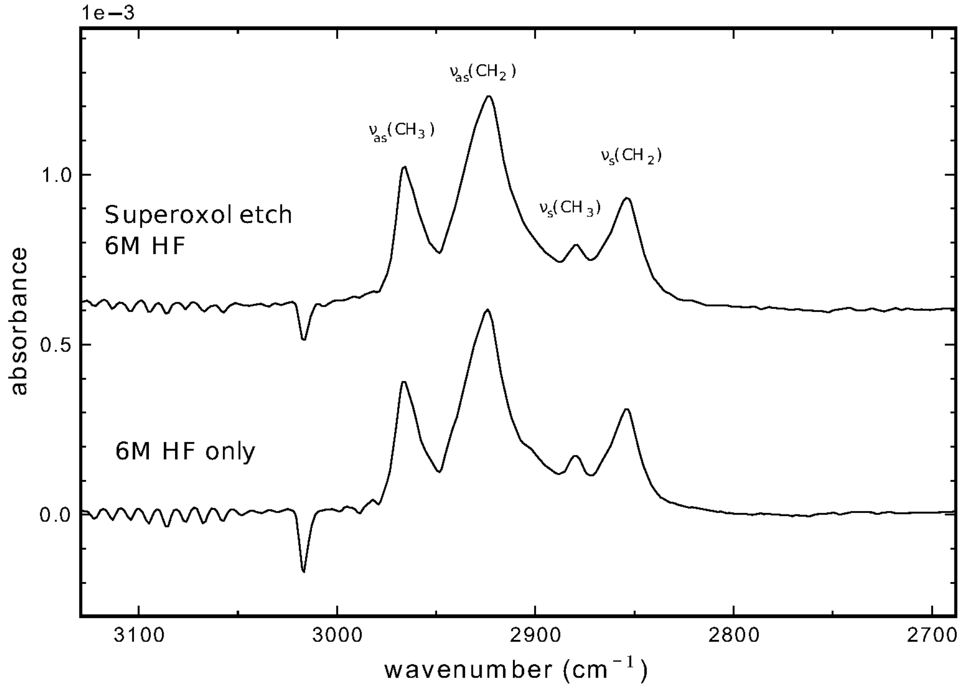

Table 5.2: Position and Full-Width at Half-Maximum[a] of Alkyl Monolayer Infrared Absorption Modes

Surface Type	Vibrational Mode	position (cm^{-1})	FWHM (cm^{-1})	orientation[b]
CH_3-Ge(111)				
	$\nu_s(CH_3)$	2906	4	$\perp$
	$\delta_s(CH_3)$	1232.5	6	$\perp$
	$\rho(CH_3)$	755	15-17	$\parallel$
CD_3-Ge(111)				
	$\nu_s(CD_3)$	2121	7	$\perp$
	$\delta_s(CD_3)$	951	5-6	$\perp$
	$\rho(CD_3)$	577	15-20	$\parallel$
$C_{10}H_{21}$-Ge(111)				
	$\nu_s(CH_3)$	2879	N/A[c]	
	$\nu_{as}(CH_3)$	2966	N/A[c]	
	$\nu_s(CH_2)$	2854	N/A[c]	
	$\nu_{as}(CH_2)$	2924	N/A[c]	
CH_3-Si(111)				
	$\nu_s(CH_3)$	2910	N/A[c]	$\perp$
	$\delta_s(CH_3)$	1256.5	6	$\perp$
	$\rho(CH_3)$	752.5	15-17	$\parallel$
CD_3-Si(111)				
	$\nu_s(CD_3)$	2128	14	$\perp$
	$\delta_s(CD_3)$	979	4-5	$\perp$
	$\rho(CD_3)$	604	12-13	$\parallel$

a for resolution of 4 cm^{-1}, incident angle of 74°

b orientation with respect to surface plane: $\perp$ = normal to the surface, $\parallel$ = parallel to the surface

c not available — asymmetric and/or had contributions from adventitious hydrocarbon

5.4 Discussion

5.4.1 Methyl-Terminated Ge(111) Surfaces

Infrared absorption spectra of CH_3-Ge(111) provide structural evidence that well-ordered monolayers of methyl groups bonded normal to the surface can be produced through the bromination/alkylation method. The peak positions of the methyl vibrational modes are lower frequency for CH_3-Ge(111) than for CH_3-Si(111), as would be expected considering the larger mass of the Ge atoms compared to Si atoms. The absorption peaks of the Ge surface were less intense than those on the Si surface, which could indicate fewer oriented methyl groups, and hence lower quality grafted layer, than that of the analogous Si surface. However, the refractive index is not the same for the two semiconductors, so only Si was truly measured at the Brewster's angle with the transmission accessory available. Because the reported angle of incidence is really an average of values defined by the cone of the narrowing IR beam, no attempt was made to normalize the peak intensity to the electric field at the surface for a fixed angle of 74 °. The similar peak width of the umbrella modes, limited by the 4 cm^{-1} resolution, is a qualitative indication that the CH_3-Ge(111) is well ordered like the CH_3-Si(111) surface.

Many variations of the halogenation/alkylation method yield modified surfaces, as evidenced by the electrical characteristics and surface elemental analysis described in earlier chapters, however not all of those procedures would yield methyl monolayers of sufficient quality to be measured by IR absorption. Pre-treatment of samples with Superoxol etch before HF etching has a noticeable effect upon the final methyl monolayer.

The lack of clear IR absorption peaks for CH_3-Ge(111) prepared from methylation of the chloride surface was not expected. While it is possible that the hydrogen-terminated surface is not ideal for alkylation, the chlorine-terminated surface would be expected to be a good surface for the reaction because it is believed to be well-ordered and has been proven to react with Grignard reagents.[16,25–28] Although the chlorinated surface produced by etching was not found to be a good precursor surface for methylation itself, it was found to be adequate if it was subsequently exposed to Br_2, as seen in Figures 5.6 and 5.7. It can also be seen in Figure 5.6 that HBr-etched surfaces can be directly methylated to form well-ordered surfaces. Samples etched with HBr and HCl were both subjected to nearly identical handling conditions, so any artifact of contamination or moisture that is independent of the nature of the halogen surface should affect both surfaces. This indicates that it is possible to directly methylate a surface that has come from an aqueous environment, and that the Br_2 vapor and Schlenk vacuum are not strictly necessary. Surfaces which had only been etched with HF prior to exposure to Br_2 did not yield IR spectra with identifiable methyl modes, so there is no evidence that the brief exposure to Br_2 etched the Ge to cause a well-ordered surface. The IR results could be explained if the Cl-Ge(111) surface reacted less preferentially with the methylmagnesium reagent over any impurities than did the Br-Ge(111), for it cannot be determined from the XPS whether all of the C 1*s* component at 284.3 B. eV is due to a methyl group or to some larger hydrocarbon impurity. To say whether the Ge-Br bond is itself necessary, it would be necessary to chlorinate the etched surfaces with Cl_2 gas. Of the surfaces studied, every successfully methylated surface had been prepared from a brominated precursor surface.

5.4.2 Etched Surfaces

The elapsed time between removal of the sample from the etchant and completion of the spectrum collection (approximately 15 min) is significantly greater than the time that the etched sample is exposed to air during the methylation procedure (less than 10 s), so that the IR spectra do not necessarily represent the precursor surface of the alkylated surfaces. The ν(Ge-H) peak is at a higher frequency than would be expected (2040 cm^{-1} vs 1970 cm^{-1} for GeH or 2020 cm^{-1} for GeH$_2$), possibly because of partial oxidation of the surface.[18,29] Nevertheless, the apparent correlation between the presence of the absorption band at 560 cm^{-1} and the smaller ν(Ge-H) peak in the pre-treated HF-etched surface and the higher quality methyl monolayer produced from such a precursor surface indicates there is at least qualitative importance to the H-Ge(111) TIRAS results.

Addition of a hydrocarbon to the HF (aq) etchant was an attempt at slowing the rate of oxidation so that the HF-etched surface could be measured. If the hydrogen-terminated surfaces are sensitive to moisture and oxygen, the hydrocarbon contaminants could adhere to the wafer surface after the oxides are removed, forming a protective layer. That assumes the hydrocarbon layer does not interact with the hydrogen-terminated surface, which may not be valid.[18] The lack of a significant ν(Ge-H) peak in either spectrum in Figure 5.12 would indicate that either the hydrogen-terminated surface had already reacted with the hydrocarbons, or that there never was a ν(Ge-H) absorption band for this surface. The presence of the 560 cm^{-1} band in the spectrum that compares the sample to itself after 50 min (the upper spectrum of Figure 5.12) indicates that the decay of the chemical species responsible for that band absorption was slowed. The addition of hydrocarbons to the HF etchant was investigated because the $NH_4Cl{-}HF$ mixed etch coated the sample with an organic contamination film, yet subsequent bromination and methylation steps produced the high-quality methyl-terminated surface as seen in Figure 5.8, indicating that organic contaminants did not necessarily interfere with the etching process.

Figure 5.11 shows ν(Ge-H) absorption bands for 12.0 M HF-etched surfaces, both pre-treated with the anisotropic etch and not pretreated. This is most likely due to surface roughening, which would negate the effects of the anisotropic etch. The total time required for the pre-treated sample to become hydrophobic in the 12.0 M HF(aq) was approximately 30 s, however the apparent transition from hydrophilic to hydrophobic was less than 5 s, which made it difficult to manually optimize the etching time. These doubts aside, both the presence of a peak at 560 cm^{-1} for the etched surface and the presence of distinct absorption bands on the methylated surface are associated with the use of the anisotropic etch. Prolonged HF-etchant exposure can lead to atomic surface roughening, so the HF-only methods of etching may yield surfaces that are too rough to allow for well-ordered methyl monolayers.[6,18]

5.4.3 Decyl-Terminated Ge(111) Surfaces

The reduction in $\nu(CH_3)$ mode absorption intensity seen in Figure 5.13 compared to Figure 5.14 indicates an anisotropic layer with the alkyl chains directed away from the surface, however the peak positions are are too high energy for crystalline alkanes, so there is some degree of disorder.[12,30] While monolayers with a more crystalline nature have been achieved on flat surfaces including Ge(100), the peak positions are in agreement with thiol- or alkane- derived monolayers on Ge(111).[15,30,31] The similarity between the spectra of the decyl layers prepared through the two different etching methods is compatible with the XPS data of alkylated surfaces, including methyl. If the etching method does not have a large impact upon the number of grafted alkyl groups per unit area and that any slight changes in chemical environment or bond orientation due to varying degrees of surface roughness would affect the carbon bonded to the top Ge, but would have less of an effect upon the hydrocarbon groups further from the surface.

5.5 Conclusion

Well-ordered CH_3-Ge(111) surfaces can be prepared via the two-step halogenation/methylation method if the appropriate etching method is employed. 6.0 M HCl or, if the surface is etched first with an HF/H_2O_2 anisotropic etchant, 6.0 M HF may be used to remove oxide prior to exposure of the surface to Br_2 vapor. Alternatively, the surface may be directly brominated with 6.0 M HBr. Exposure of the HCl-etched or HF-etched surface directly to CH_3MgX (X=Cl,Br,I,CH_3) results in a hydrophobic, oxidation resistant surface, but characteristic IR absorption peaks cannot be detected.

The methyl umbrella mode and methyl rocking mode are similar to what is observed with CH_3-Si(111), but at lower frequency. The umbrella mode absorption peak is dependent upon the wafer orientation with respect to the incident infrared beam, indicating the vibration mode is normal to the surface.

In contrast to what was observed with the CH_3-Ge(111) case, $C_{10}H_{21}$-Ge(111) surfaces prepared with or without the anisotropic etch prior to 6.0 M HF etch yielded nearly identical IR spectra. The packing density and degree of order in the hydrocarbon monolayer is not as sensitive to the initial surface quality as the more restricted methyl monolayer.

Bibliography

[1] Webb, L.; Rivillon, S.; Michalak, D.; Chabal, Y.; Lewis, N. *J. Phys. Chem. B* **2006**, *110*, 7349–7356.

[2] Yu, H.; Webb, L.; Heath, J.; Lewis, N. *Appl. Phys. Lett.* **2006**, *88*, 252111.

[3] Hunger, R.; Fritsche, R.; Jaeckel, B.; Jaegermann, W.; Webb, L.; Lewis, N. *Phys. Rev. B* **2005**, *72*, 045317.

[4] Rivillion, S.; Chabal, Y. *J. Phys. IV* **2006**, *132*, 195–198.

[5] Sharp, I.; Schoell, S.; Hoeb, M.; Brandt, M.; Stutzmann, M. *Appl. Phys. Lett.* **2008**, *92*, 223306.

[6] Choi, K.; Buriak, J. *Langmuir* **2000**, *16*, 7737–7741.

[7] Ardalan, P.; Sun, Y.; Pianetta, P.; Musgrave, C. B.; Bent, S. F. *Langmuir* **2010**, *26*, 8419–8429.

[8] `http://eom.umicore.com/en/materials/library/brochuresAndMarketingMaterial/GermaniumOpticsBrochure.pdf`.

[9] `http://www.harricksci.com/~harrcov7/silicon`.

[10] Greenler, R. *J. Chem. Phys.* **1966**, *44*, 310–315.

[11] Mielczarski, J.; Yoon, R. *J. Phys. Chem.* **1989**, *93*, 2034–2038.

[12] Hoffmann, H.; Mayer, U.; Krischanitz, A. *Langmuir* **1995**, *11*, 1304–1312.

[13] Brunner, H.; Mayer, U.; Hoffmann, H. *Appl. Spectr.* **1997**, *51*, 209–217.

[14] Chernyshova, I.; Rao, K. *J. Phys. Chem. B* **2001**, *105*, 810–820.

[15] Kosuri, M.; Cone, Q., R. Li; S.M., H.; Bunker, B.; Mayer, T. *Langmuir* **2004**, *20*, 835–840.

[16] Lu, Z. *Appl. Phys. Lett.* **1996**, *68*, 1996.

[17] Zahler, J.; Fontcuberta i Morral, A.; Griggs, M.; Atwater, H. A.; Chabal, Y. J. *Phys. Rev. B* **2007**, *75*, 035309.

[18] Rivillion, S.; Chabal, Y. J.; Amy, F.; Kahn, A. *Appl. Phys. Lett.* **2005**, *87*, 253101.

[19] Lauwaert, J.; De Baerdemaeker, J.; Dauwe, C.; Clauws, P. *J. Mater. Sci.: Mater. Electron.* **2007**, *18*, 793–797.

[20] Jobson, K.; Wells, J.-P.; Schropp, R.; Vinh, N.; Dijkhuis, J. *J. Appl. Phys.* **2008**, *103*, 013106.

[21] Ferguson, K., G.A.and Raghavachari; Michalak, D.; Chabal, Y. *J. Phys. Chem. C* **2008**, *112*, 1034–1039.

[22] Hellstrom, P.; Holmgren, A.; Oberg, S. *J. Phys. Chem. C* **2007**, *111*, 16920–16926.

[23] Linford, M.; Fenter, P.; Eisenberger, P.; Chidsey, C. *J. Am. Chem. Soc.* **1995**, *117*, 3145–3155.

[24] Scheres, L.; Giesbers, M.; Zuilhof, H. *Langmuir* **2009**, *26*, 4790–4795.

[25] Amick, J.; Cullen, G.; Gerlich, D. *J. Electrochem. Soc.* **1962**, *109*, 127–132.

[26] He, J.; Lu, Z.; Mitchell, S.; Wayner, D. *J. Am. Chem. Soc.* **1998**, *120*, 2660–2661.

[27] Cao, S.; Tang, J.-C.; Wang, L.; Zhu, P.; Shen, S. *Surf. Sci.* **2002**, *505*, 289–294.

[28] Wang, D.; Dai, H. *Appl. Phys. A* **2006**, *85*, 217–225.

[29] Maroun, F.; Ozanam, F.; Chazalviel, J.-N. *J. Phys. Chem. B* **1999**, *103*, 5280–5288.

[30] Porter, M.; Bright, T.; Allara, D.; Chidsey, C. *J. Am. Chem. Soc.* **1987**, *109*, 3559–3568.

[31] Ardalan, P.; Musgrave, C.; Bent, S. *Langmuir* **2009**, *25*, 2013–2025.